International Journal of Heat and Mass Transfer 52 (2009) 3473–3480

Contents lists available at ScienceDirect

International Journal of Heat and Mass Transfer

journal homepage: www.elsevier.com/locate/ijhmt

Numerical study of the heat sink with un-uniform fin width designs

Yue-Tzu Yang *, Huan-Sen Peng

Department of Mechanical Engineering, National Cheng Kung University, Tainan 70101, Taiwan

ARTICLE INFO

Article history:
Received 27 June 2008
Received in revised form 13 February 2009
Accepted 13 February 2009
Available online 22 April 2009

Keywords:
Heat sink
Un-uniform fin width design
Electronics cooling
CFD

ABSTRACT

The thermal performances of the heat sink with un-uniform fin width designs with an impingement cooling were investigated numerically. The governing equations are discretized by using a control-volume-based finite-difference method with a power-law scheme on an orthogonal non-uniform staggered grid. The coupling of the velocity and the pressure terms of momentum equations are solved by the SIMPLEC algorithm. The well-known $k-\varepsilon$ two-equations turbulence model is employed to describe the turbulent structure and behavior. The parameters include the five Reynolds number (Re = 5000–25000), three fin heights (H = 35, 40, 45 mm), and five fin width designs (Type-1–Type-5). The objective of this study is to examine the effects of the fin shape of the heat sink on the thermal performance. The results show that the Nusselt number increases with the Reynolds number. The increment of the Nusselt number decreases gradually with the increasing Reynolds number. Furthermore, the effects of fin dimensions on the Nusselt number at high Reynolds numbers are more significant than that at low Reynolds numbers. It is also found that there is potential for optimizing the un-uniform fin width design.

1. Introduction

With the rapid development of electronic technology, electronic appliances and devices now are always in our daily life. Under the condition of multifunction, high clock speed, shrinking package size, and higher power dissipations, the heat flux per unit area increased dramatically over the past few years. In addition, the working temperature of the electronic components may exceed the desired temperature level. Thus, an efficient cooling and maintaining the die at a reasonable operating temperature have played an important role in insuring a reliable operation of electronic components.

There are many methods in electronics cooling, such as jet impingement cooling [1,2], heat sink [3], microchannel heat sink [4], and heat pipe [5–7], etc. Conventional electronics cooling normally used impinging jet with heat sink showing superiority in terms of unit price, weight and reliability. Therefore, the most common way to enhance the air-cooling is through the utilization of impinging air jets on a heat sink. In order to design an effective heat sink, some criterions such as a large heat transfer rate, a low pressure drop, an easier manufacturing, a simpler structure, a reasonable cost and so on should be considered.

A number of research scholars have examined the thermal and hydraulic characteristics of various heat sinks extensively. The steady-state forced-convection cooling of a horizontally based pin-fin assembly has been investigated experimentally by Haq et al. [8]. The overall pressure drop and the effect of the shroud clearance were examined. Ledezma et al. [9] performed an experimental, numerical and theoretical study of the heat transfer on a pin-finned plate. They carried out the correlation equations for an optimal fin-to-fin spacing and a maximum thermal conductance. Brignoni and Garimella [10] demonstrated the experimental optimization of confined impinging air jets used in conjunction with a pin-fin heat sink. Enhancement factors for the heat sink were evaluated, and the range of 2.8–9.7 was obtained relative to a bare surface. Both the average heat transfer coefficients and the thermal resistance were expressed for the heat sink as a function of a Reynolds number, an air flow rate, a pumping power, and a pressure drop, to assist in optimizing the jet impingement configuration for given design constraints. Maveety and Hendricks [11] showed a performance study of pin-fin heat sinks with impingement cooling which considered the effects of geometry, nozzle-to-heat sink vertical placement, material, and the Reynolds number. The results revealed that the best performance occurred when the dimensionless impingement distance was between 8 and 12, and when the Reynolds number was between 40000 and 50000. The results also presented that due to the higher spreading resistance efficiency of the carbon composite material, it led to a more uniform cooling of the heat sink. Moreover, the influence of the nozzle-to-heat sink vertical placement on the thermal performance was reduced as the Reynolds number increased. Maveety and Jung [12] have investigated the comparisons between computational and experimental results for the cooling performance from a pin-fin heat sink with an impinging air flow. Furthermore, optimization studies were discussed to quantify the effects of changing

* Corresponding author. Tel.: +886 6 2757575 x 62172; fax: +886 6 2352973.
E-mail address: ytyang@mail.ncku.edu.tw (Y.-T. Yang).

0017-9310/$ - see front matter © 2009 Elsevier Ltd. All rights reserved.
doi:10.1016/j.ijheatmasstransfer.2009.02.042

Nomenclature

A_h	heating area (m^2)
b	thickness of the base of the heat sink (mm)
C_1, C_2, C_μ	turbulent constant
COE	coefficient of enhancement
d	diameter of the nozzle (m)
h	heat transfer coefficient based on A_h (W/m^2K)
H	height of the fins (mm)
k	turbulent kinetic energy (m^2/s^2)
k_a	thermal conductivity of air (W/mK)
k_s	thermal conductivity of aluminum alloy (W/mK)
L	length of the base of the heat sink (mm)
Nu	Nusselt number ($=hd/k_a$)
p	pressure (N/m^2)
Q	heating power (W)
Re	Reynolds number ($=\|V_{in}\|d/v$)
R_{th}	thermal resistance (K/W)
T	temperature (K)
u_i, u_j	velocity component (m/s)
V	velocity in the Y-direction (m/s)
W	width of the fins (mm)
x_i, x_j	coordinates (m)

Greek symbols

ε	turbulent energy dissipation rate (m^2/s^2)
μ	dynamic viscosity (Ns/m^2)
v	kinematic viscosity (m^2/s)
ρ	density (kg/m^3)
σ	Prandtl number
σ_k, σ_ε	turbulent constant

Subscripts

ave	average
base	base
film	film
in	inlet
l	laminar
new	new design
origin	original design
t	turbulent

the fin length and the fin cross-sectional area on the cooling performance. The numerical results illustrated a complex pressure gradient inside the fin array and a greater pressure gradient improved mixing and heat transfer. Their simulations also demonstrated a complicated fluid motion with large pressure gradients that generated vorticity, circulation and flow reversals. The enhancement of heat transfer from a discrete heat source in a confined air jet impingement was experimentally studied by El-Sheikh and Garimella [13]. Relative to an unpinned heat sink, the heat transfer from the pinned ones improved by 2.4–9.2 times. Due to the introduction of the heat sinks, the enhancement factors relative to the bare heat source varied from 7.5 to 72. Results for the average heat transfer coefficient were correlated as a function of the Reynolds number, fluid properties and geometric parameters of the heat sinks. Hwang and Lui [14,15] studied the heat transfer and pressure drop characteristics between pin-fin trapezoidal ducts with straight and lateral outlet flows. The effect of pin arrangement for the ducts of different direction outlet flow was also examined. Moreover, a similarity of the pin Reynolds number dependence of row-averaged Nusselt number was developed. An experimental study was conducted to investigate the heat transfer from a parallel flat plate heat sink under a turbulent air jet impingement by Sansoucy et al. [16]. The forced convection heat transfer rates from a flat plate and from a flat plated heat sink under an impinging confined jet have been obtained. In addition, the experimental results were compared with the numerical predictions obtained in an earlier study. They concluded that the numerical analysis in a previous study was adequate for appraising the mean heat transfer rate in jet impingement for situations of thermal management of electronics. Chiang and Chang [17] and Chiang et al. [18] developed the response surface methodology (RSM) and applied grey-fuzzy logic to find the optimal values of designing parameters of a pin-fin type heat sink under constrains of mass and space limitations to achieve the high thermal performance. The optimal designing parameters have been carried out and verified by conducting confirmation experiments. Li et al. [19] and Li and Chen [20] investigated the thermal performance of pin-fin and plate-fin heat sinks with confined impingement cooling by using infrared thermography. The results show that the thermal resistance of the heat sinks decreases with the increased Reynolds number of the impinging jet. However, the reduction of the thermal resistance decreases gradually as the Reynolds number increases. Moreover, it revealed that the influence of fin width is more obvious than the fin height. In addition, the optimal impinging distance increases with the increasing Reynolds number. Finally, they concluded that the thermal performance of the pin-fin heat sinks is superior to that of the plate-fin heat ones. Furthermore, the thermal performance of pin-fin heat sinks with air impingement cooling was performed numerically and experimentally by Li and Chen [21]. The effects of the fin geometry and the Reynolds number on the heat transfer of the heat sinks were discussed, as well. The experimental investigation of plate-fin and pin-fin heat sinks was conducted by Kim et al. [22]. They compared the thermal performance of these two types of heat sinks and obtained the correlations for the pin-fin heat sinks. The thermal and hydraulic behavior due to jet impingement on pin-fin heat sinks was experimentally investigated by Issa and Ortega [23]. This study showed that the pressure loss coefficient increased with increasing pin density and pin diameter, and decreased with increasing pin height and clearance ratio. Moreover, the overall base-to-ambient thermal resistance decreased with increasing Reynolds number, pin density and pin diameter.

Excluding numerical simulation or experimental studies, the entropy generation method was also utilized to evaluate or optimize the thermal performance of the heat sink [24–28]. The procedure is based on the minimization of entropy generation resulting from heat transfer and pressure drop. The model demonstrates a rapid and stable procedure for obtaining optimum design/operational conditions without resorting to parametric analysis by using repeated iterations with a thermal analysis tool.

Moreover, some scholars have interests in altering the fin shape to enhance the thermal and hydraulic performance. Lorenzini and Moretti [29] analyzed the Y-shape fins and examined the geometries by varying the angle between the two arms of the Y and proposed new shape for the fins. Naphon and Sookkasem [30] investigated the heat transfer characteristics of tapered cylinder pin-fin heat sinks experimentally and numerically. Ledezma and Bejan [31] performed the experimental and numerical study of heat sinks with sloped plate fins. This study discussed the thermal performance on the orientation of the fin array and the tilting of the crests of the plate fins. Ji et al. [32] studied the cooling perfor-

mance of triangular folded fin heat sink. They discussed the influence of the fin pitch, the Reynolds number, and the fin height. The results showed that the cooling performance of triangular folded fin heat sinks depended significantly on the fin height, the fin pitch, and the Reynolds number. Moreover, the empirical correlations were developed to predict the heat transfer coefficient and pressure drop. Sathe and Sammakia [33] presented a study of a new and unique high-performance air-cooled impingement heat sink. The comparisons between numerical simulations and experimental data of the heat sink performance have been conducted. The effects of the fin thickness, inter-fin gap, nozzle width, and fin shape on the heat transfer and pressure drop have been studied. The study showed that the pressure drop can be decreased by cutting the fins in the central impingement zone without sacrificing heat transfer rates. The numerical predictions of heat transfer and flow characteristics of heat sinks with ribbed and dimpled surface have been done by Wee et al. [34]. The results showed that the heat transfer augmentation produced by the ribs is about 104% higher than that produced by the smooth-surface heat sink. But the ribs also produce higher static pressure variations, higher velocity gradients, and higher streamwise vorticity magnitudes. Applying dimples to heat sink surface gives a spatially averaged Nusselt number increase of 63%, with a pressure drop penalty which is much lower than the one produced by ribbed surfaces. Shah et al. [35] demonstrated the results of a numerical analysis of the performance of an impingement heat sink designed for use with a specific blower as a single unit. The effects of the shape of the heat sink fins, particularly near the center of the heat sink were examined. It is found that the removal of fin material from the central region of the heat sink enhances the thermal as well as the hydraulic performance of the sink. Shah et al. [36] extends the previous work by investigating the effect of the removal of a fin material from the end fins, the total number of fins, and the reduction in the size of the hub fan. The reduction in the size of the hub of the fan is found to be a more uniform distribution of the air inside the heat sink, particularly near the center of the module. Increasing the number of fins indicates a small drop in the temperature, accompanied by a significant pressure rise. Moreover, they reported a new optimal heat sink design by employing the actual fan operating characteristics.

Generally speaking, there are many testing processes for heat sinks which must be introduced in an effort to obtain the thermal and hydraulic performance of heat sinks. If we take advantage of the numerical simulation to acquire some probable optimal design parameters before running experiments, the cost and research time can be reduced. In this paper, the numerical simulation of pin-fin heat sinks with impingement cooling in thermal-fluid characteristics will be investigated. The purpose of this study is to examine the effect of the fin shape on the thermal performance of the heat sink.

2. Mathematical model and numerical method

The schematic diagram of the geometry and the computational domain is shown in Fig. 1. The turbulent three-dimensional Navier–Stokes and energy equations are solved numerically (using a finite-difference scheme) combined with the continuity equation to simulate the thermal and turbulent flow fields. An eddy viscosity model is used to account for the effects of turbulence. The flow is assumed to be steady, incompressible, and three-dimensional. The buoyancy and radiation heat transfer effects are neglected. In addition, the thermophysical properties of the fluid are assumed to be constant.

The three-dimensional governing equations of mass, momentum, turbulent kinetic energy, turbulent energy dissipation rate, and energy in the steady turbulent main flow using the standard $k-\varepsilon$ model are as follows:

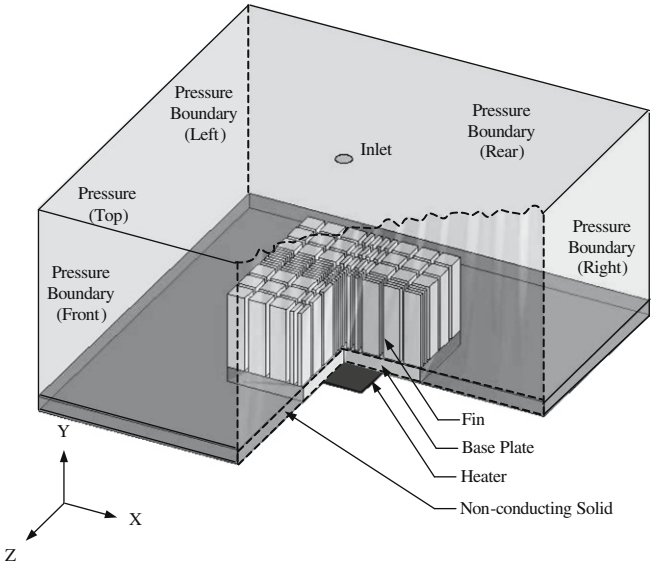

Fig. 1. Physical domain.

(1) Continuity equation

$$\frac{\partial \rho \bar{u}_i}{\partial x_i} = 0 \tag{1}$$

(2) Momentum equation

$$\rho \bar{u}_j \frac{\partial \bar{u}_i}{\partial x_j} = -\frac{\partial \bar{p}}{\partial x_i} + \frac{\partial}{\partial x_j}\left[\mu_t\left(\frac{\partial \bar{u}_i}{\partial x_j} + \frac{\partial \bar{u}_j}{\partial x_i}\right)\right] \tag{2}$$

(3) Energy equation

$$\rho \bar{u}_j \frac{\partial \overline{T}}{\partial x_j} = -\frac{\partial}{\partial x_j}\left[\left(\frac{\mu_l}{\sigma_l} + \frac{\mu_t}{\sigma_t}\right)\frac{\partial \overline{T}}{\partial x_j}\right] \tag{3}$$

(4) Transport equation for k

$$\rho \bar{u}_j \frac{\partial k}{\partial x_j} = \frac{\partial}{\partial x_j}\left(\frac{\mu_t}{\sigma_k}\frac{\partial k}{\partial x_j}\right) + \mu_t\left(\frac{\partial \bar{u}_i}{\partial x_j} + \frac{\partial \bar{u}_j}{\partial x_i}\right)\frac{\partial \bar{u}_i}{\partial x_j} - \rho\epsilon \tag{4}$$

(5) Transport equation for ε

$$\rho \bar{u}_j \frac{\partial \epsilon}{\partial x_j} = \frac{\partial}{\partial x_j}\left(\frac{\mu_t}{\sigma_\epsilon}\frac{\partial \epsilon}{\partial x_j}\right) + C_1 \mu_t \frac{\epsilon}{k}\left(\frac{\partial \bar{u}_i}{\partial x_j} + \frac{\partial \bar{u}_j}{\partial x_i}\right)\frac{\partial \bar{u}_i}{\partial x_j} - C_2 \rho \frac{\epsilon^2}{k} \tag{5}$$

The empirical constants appear in the above equations are given by the following values: $C_1 = 1.44$, $C_2 = 1.92$, $C_\mu = 0.09$, $\sigma_k = 1.0$, $\sigma_\varepsilon = 1.3$

The governing equation for the solid can be written as:

$$\frac{\partial}{\partial x_i}\left(k_s \frac{\partial T}{\partial x_i}\right) = 0 \tag{6}$$

The Reynolds number of the impinging jet is defined as

$$Re = \frac{|V_{in}|\, d}{\nu} \tag{7}$$

where d denotes the diameter of nozzle.

The average convection heat transfer coefficient h is calculated by

$$h = \frac{Q}{A_h(T_{base} - T_{in})} \tag{8}$$

The average Nusselt number Nu is calculated by

$$Nu = \frac{hd}{k_a} \tag{9}$$

Following the definition given in Sansoucy et al. [16], the coefficient of enhancement (COE) is defined to quantify the improvement in heat transfer rates due to the different types of the heat sink fins. This is expressed as

$$\mathrm{COE} = \frac{Nu_{new}}{Nu_{origin}} \tag{10}$$

where k_a is evaluated at the film temperature $T_{film}\left(T_{film} = \frac{T_{base}+T_{in}}{2}\right)$

The thermal resistance of the heat sink is calculated by

$$R_{th} = \frac{T_{ave} - T_{in}}{Q} \tag{11}$$

The dimensions of the computational domain were based on the work by Li and Chen [21]. Taking advantage of the symmetry, the numerical simulations have been performed by considering only a one-quarter model of the physical domain. The boundary conditions for this problem are stated as follows. At the flow inlet, the air was uniformly induced downward with a constant temperature. The pressure boundary conditions are used at the outlet. No slip conditions with thermally insulated are provided on all the other walls. At the bottom of the heat sink, a uniform constant heat flux is applied on the heating area. The adiabatic thermal boundary conditions are utilized at the outer perimeter of the bottom of heat sink except for the heating area. In addition, because of symmetric assumptions only a quarter of a heat sink and a quarter of channel are calculated as shown in Fig. 2.

A non-uniform and staggered grid system with a large concentration of nodes in regions of steep gradients, such as those close to the walls was employed. A staggered grid arrangement is used in which the velocities are stored at a location on the control-volume faces. All other variables including pressure are calculated at the grid points. The numerical method used in the present study is based on the SIMPLEC (Semi-Implicit Method for Pressure-Linked Equation Consistent) algorithm of van Doormaal and Raithby [37]. Pressure and velocity correction schemes are implemented in the model algorithm to arrive at a converged solution when both the pressure and velocity satisfy the momentum and continuity equations. For non-linear problems, under-relaxation is employed to avoid divergence in the iterative solutions. The resulting sets of discretized equations for each variable are solved by the line-by-line procedure which is the combination of the Tri-Diagonal Matrix Algorithm (TDMA) and the Gauss–Seidel iteration technique of Patankar [38]. The solution is considered to be converged when the normalized residual of the algebraic equation is less than a prescribed value of 10^{-3}.

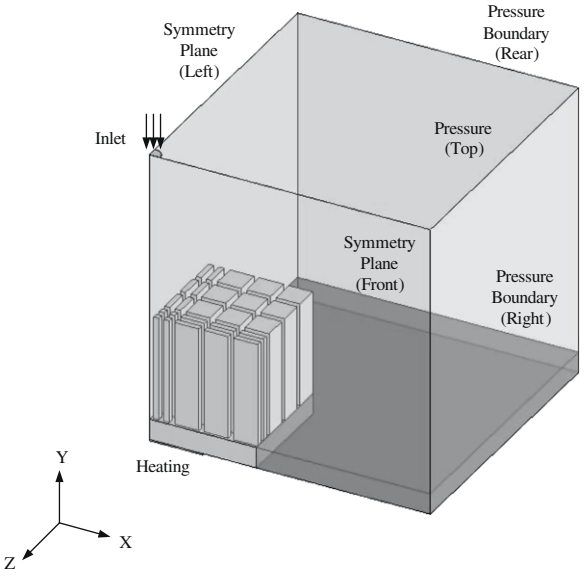

Fig. 2. Computational domain and boundary conditions.

3. Results and discussion

The denotations and dimensions of the aluminum heat sinks with different un-uniform fin width designs in this study are depicted in Fig. 3 and Table 1. The effects of the impinging Reynolds number and the fin dimensions on the thermal performance are investigated. The parameters used in this study include five Reynolds numbers (Re = 5000–25000), three fin heights (H = 35, 40, 45 mm), and five fin width designs (Type-1–Type-5). Fig. 4 shows the configuration of the heat sinks. The heat sink comprises a 10×10 array of fins. The width of inter-fin spacing is constant. The material of heat sink is selected as aluminum alloy 6061 and has a value 168 W/mK in thermal conductivity. Both the length and width of the base of the heat sink are 80 mm. The area of the heater is 40×40 mm, which is in the center of the heat sink. The heating area is heated with heating power 20 W.

3.1. Verification

In order to verify the present numerical model, the thermal resistance of the heat sink comprises a 6×6 array of uniform width of the fins (W = 8.0 mm) under the conditions Re = 5000 ~ 25000 and Q = 20 W, which are compared with Li and Chen [21] as shown in Fig. 5. Moreover, a total number of cells, 61357, 85713 and 120374 were employed to assess the grid independence as shown in Fig. 6. The deviations of the Nusselt number predicted using meshes with 61357 and 85713 cells are 1.5% and 0.5% from the obtained using a mesh with 120374 cells. The results

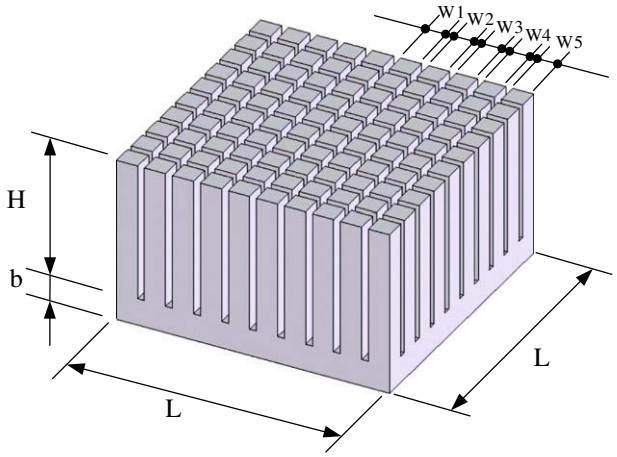

Fig. 3. Geometry of heat sink (Type-3, original design).

Table 1
Dimensions of the fins.

Fin shape	Fin width				
	$W1$ (mm)	$W2$ (mm)	$W3$ (mm)	$W4$ (mm)	$W5$ (mm)
Type-1	2.0	2.0	9.0	9.0	9.0
Type-2	5.0	5.0	7.0	7.0	7.0
Type-3	6.2	6.2	6.2	6.2	6.2
Type-4	8.0	8.0	5.0	5.0	5.0
Type-5	11.0	11.0	3.0	3.0	3.0

L = 80 mm, b = 8.0 mm.

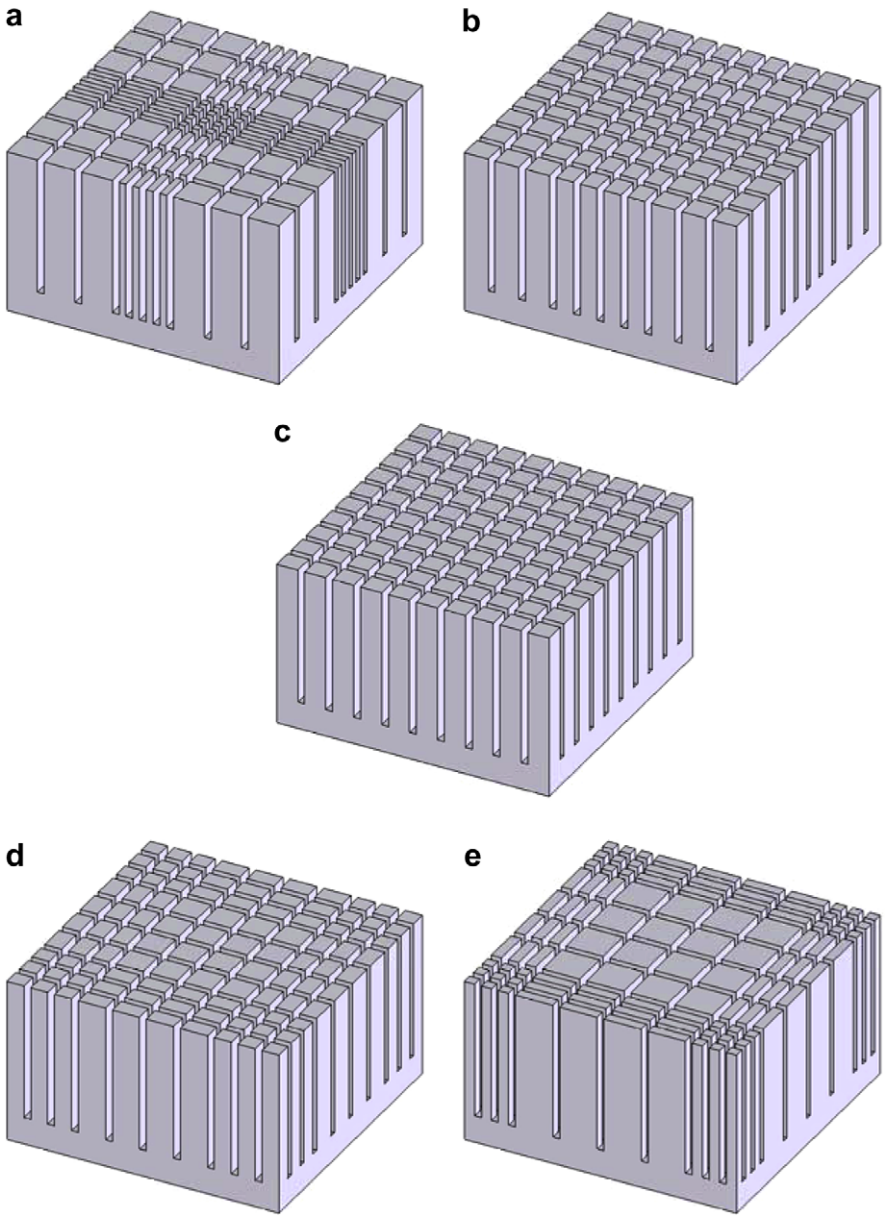

Fig. 4. Schematic diagram showing different fin width designs in the study (a) Type-1 (b) Type-2 (c) Type-3 (d) Type-4 (e) Type-5.

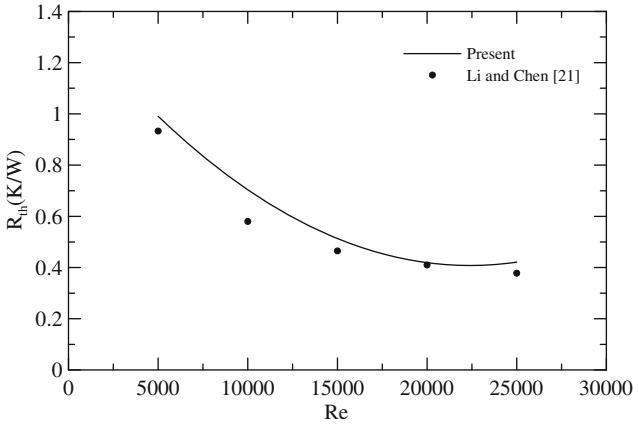

Fig. 5. Verification of numerical model.

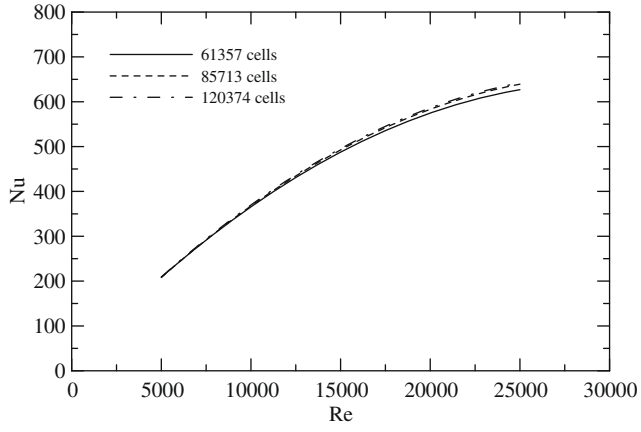

Fig. 6. Grid independent test.

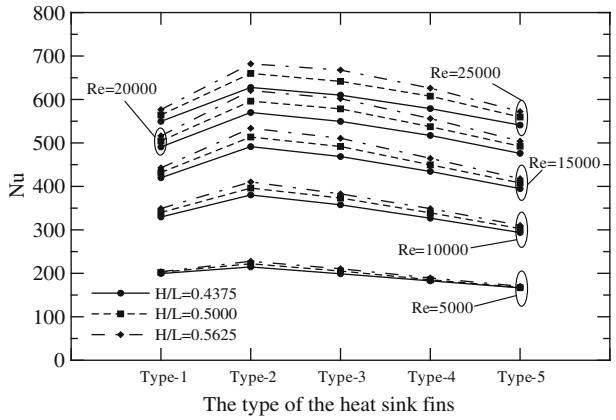

Fig. 7. Effects of the impinging Reynolds number and the fin dimensions on Nusselt number.

of the grid sensitivity study showed that the simulations based on the 85713 meshes provide satisfactory numerical accuracy. Besides, the average error between simulation results and experimental data is about 10%. Reasonable discrepancies between numerical calculations and the available experimental results of Li and Chen [21] may be caused by the isotropic assumption, numerical error or 9.1% uncertainty of Li and Chen [21].

3.2. Effects of the impinging Reynolds number and the fin dimensions

The Nusselt number of the heat sink with various fin dimensions and impinging Reynolds numbers are shown in Fig. 7. As the figure indicates, the Nusselt number increases with the increasing Reynolds number. However, the increment of the Nusselt number decreases gradually as the Reynolds number increases. Moreover, the Nusselt number also increases with the increasing fin height. Increasing the height of the fins enlarges the heat transfer area of the heat sink, which enhances the heat transfer rate. The influences of the fin height on the Nusselt number at high Reynolds numbers are more obvious than that at low Reynolds numbers. The trends of the curves also show that the Nusselt number of the Type-2 design is higher than the others.

3.3. Effects of the fin width design

The effects of the fin width design on pressure field are given in Fig. 8. It can be seen that the pressure fields show the obviously variations neat the tips of the central fins and the stagnation region. The flow in the axial direction is decelerated giving rise to increase static pressure at the impingement region. When the fin design change from Type-1 to Type-2, the pressure at the stagnation point decreases. The flow resistance of Type-1 at the central region of the heat sink is lower than Type-2. This makes the variation of velocity of Type-1 from the tip of fins towards the bottom

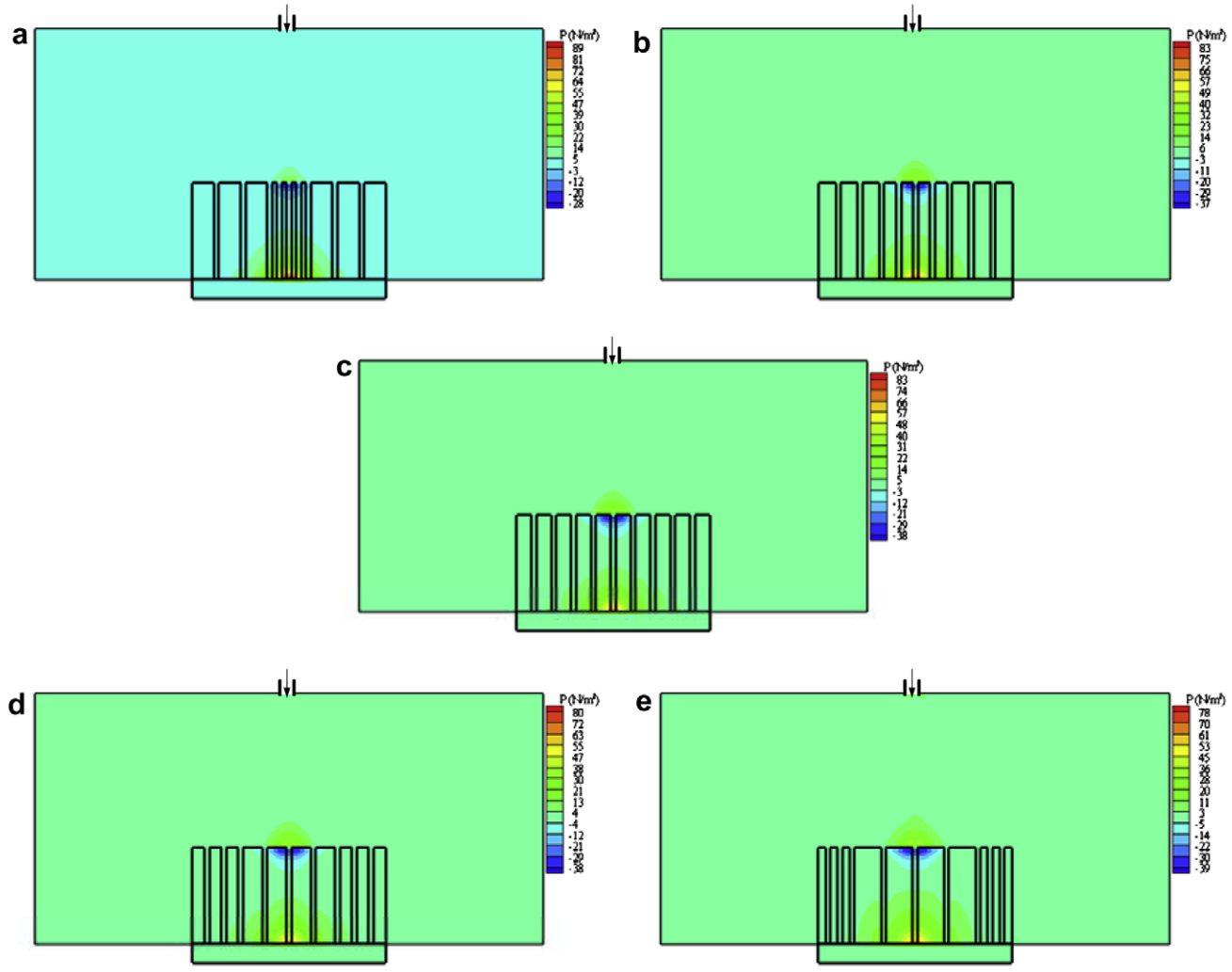

Fig. 8. Effects of the fin width design on pressure field (Re = 10000, H/L = 0.5000, middle cross section of the heat sink) (a) Type-1 (b) Type-2 (c) Type-3 (d) Type-4 (e)Type-5.

higher than Type-2. Hence, at the stagnation point, the pressure of Type-1 is higher than Type-2. As the fin design changes from Type-2 to Type-3, Type-4 and Type-5, the pressure still decreases, which is similar to the previous condition.

Fig. 9 depicts the effects of the different fin width designs on the Nusselt numbers. As seen in this figure, the Nusselt number increases with the increasing Reynolds number. The increment of the Nusselt number decreases gradually with the increasing Reynolds number. Besides, the decrease of the increment of the Nusselt number of Type-1 is more obvious than other designs. As seen in Fig. 9(a), only Type-2 is superior to Type-1 at $Re = 5000$. With the increasing Reynolds number, Type-3 and Type-4 exceed Type-1 gradually. From this figure, we may reasonably conclude that the Tyep-5 will exceed Type-1 at higher Reynolds numbers. The trends of Fig. 9(b) and Fig. 9(c) are similar to Fig. 9(a) except for the condition at $Re = 5000$. At $Re = 5000$, the Nusselt number of Type-3 is higher than Type-1 under the conditions $H/L = 0.5000$ and $H/L = 0.5625$. The temperature in the center of the heat sink is much higher than all other areas. Therefore, it is important to enlarge the heat transfer area and the flow rate for the efficient heat dissipation in the central region of the heat sink. However, the flow penetration into the heat sink is weak at low Reynolds numbers. Accordingly, the cut of flow channel should be congregated in the center of the heat sink to reduce the flow resistance in the central region. More working fluid could flow into the center of the heat sink instead of bypassing them to enhance

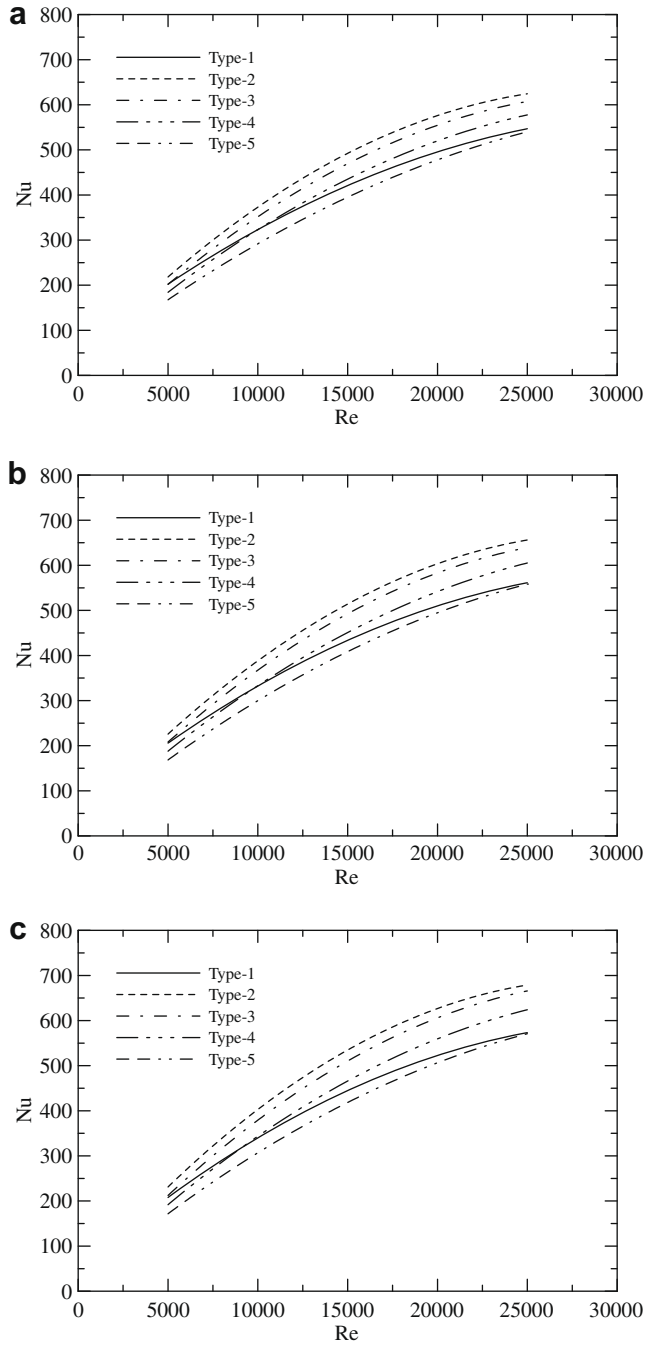

Fig. 9. Effects of the impinging Reynolds number and the fin width design on Nusselt number (a) $H/L = 0.4375$ (b) $H/L = 0.5000$ (c) $H/L = 0.5625$.

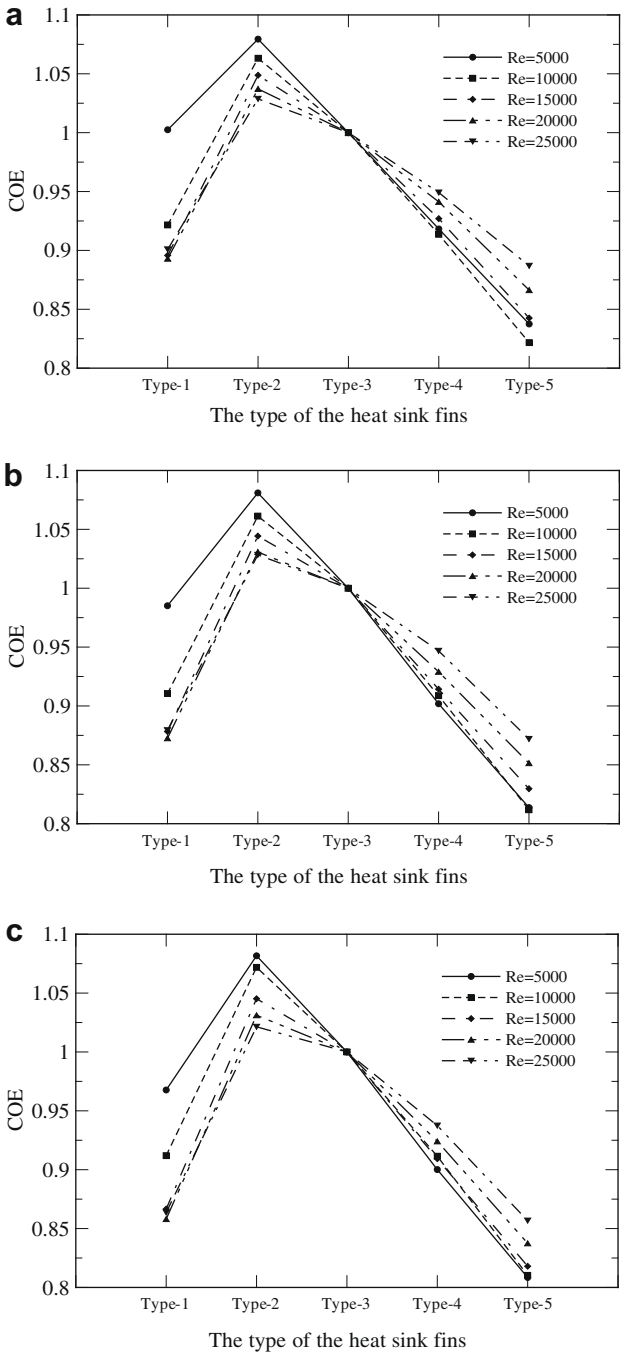

Fig. 10. Effects of the impinging Reynolds number and the fin width design on COE (a) $H/L = 0.4375$ (b) $H/L = 0.5000$ (c) $H/L = 0.5625$.

the heat transfer rate. Although the design of Type-1 could allow more working fluid flows into the center of the heat sink, the fins in the central region is too thin to dissipate heat efficiently. Therefore, the Nusselt number of Type-1 is lower than Type-2. By increasing the Reynolds number, the penetration of the working fluid becomes stronger. Hence, Type-3 and Type-4 are exceeding Type-1 gradually.

Fig. 10 shows the effects of different fin width designs on the COE. The COE is calculated based on the original design (Type-3, uniform fin width). It can be seen that COE increases when the fin shape changes from Type-1 to Type-2. When the fin shape changes from Type-2 to Type-3, the COE decreases. As the fin shape changes from Type-3 to Type-4 or Type-5, the COE decreases, similar to the previous condition. Moreover, the present results also reveal that the COE of Type-2 is higher than all the other designs.

4. Conclusion

The numerical simulation of the heat sink with an impingement cooling at various Reynolds numbers and fin dimensions are proposed. The purpose of this study is to evaluate the possibility of improving the thermal performance by utilizing the un-uniform fin width design of the heat sink. It is found that an adequate un-uniform fin width design could increase the Nusselt number and the COE of the heat sink simultaneously. Besides, the increment of the Nusselt number decreases gradually as the Reynolds number increases. The enhancement of the heat transfer by increasing the Reynolds number of the impinging jet may have a limitation. Moreover, the effects of fin dimensions on the Nusselt number at high Reynolds numbers are more obvious than that at low Reynolds numbers. In addition, the results also show that there is potential for optimizing the un-uniform fin width design.

Acknowledgements

The support of the National Science Council (NSC) of Taiwan under contract No. NSC 96-2221-E-006-161-MY2 is gratefully acknowledged. The authors also thank the National Center for High-Performance Computing (NCHC) for computer time and facilities.

References

[1] Y.M. Chung, K.H. Luo, Unsteady heat transfer analysis of an impinging jet, Transactions of the ASME, J. Heat Transfer 124 (2002) 1039–1048.
[2] K. Nishino, M. Samada, K. Kasuya, K. Torii, Turbulence statistics in the stagnation region of an axisymmetric impinging jet flow, Int. J. Heat Fluid Flow 17 (1996) 193–201.
[3] H. Jonsson, B. Moshfegh, Modeling of the thermal and hydraulic performance of plate fin, strip fin, and pin fin heat sinks-influence of flow bypass, IEEE Trans. Compon. Packaging Technol. 24 (2) (2001) 142–149.
[4] Z.G. Li, X.L. Huai, Y.J. Tao, H.Z. Chen, Effects of thermal property variations on the liquid flow and heat transfer in microchannel heat sinks, Appl. Therm. Eng. 27 (2007) 2803–2814.
[5] K.S. Kim, M.H. Won, J.W. Kim, B.J. Back, Heat pipe cooling technology for desktop PC CPU, Appl. Therm. Eng. 23 (2003) 1137–1144.
[6] Y. Wang, K. Vafai, An experimental investigation of the thermal performance of an asymmetrical flat plate heat pipe, Int. J. Heat Mass Transfer 43 (2000) 2657–2668.
[7] Z. Zhao, C.T. Avedisian, Enhancing forced air convection heat transfer from an array of parallel plate fins using a heat pipe, Int. J. Heat Mass Transfer 40 (13) (1997) 3135–3147.
[8] R.F.B. Haq, K. Akintunde, S.D. Probert, Thermal performance of a pin-fin assembly, Int. J. Heat Fluid Flow 16 (1995) 50–55.
[9] G. Ledezma, A.M. Morega, A. Bejan, Optimal spacing between pin fins with impinging flow, Transactions of the ASME, J. Heat Transfer 118 (1996) 570–577.
[10] L.A. Brignoni, S.V. Garimella, Experimental optimization of confined air jet impingement on a pin fin heat sink, IEEE Trans. Compon. Packaging Technol. 22 (3) (1999) 399–404.
[11] J.G. Maveety, J.F. Hendricks, A heat sink performance study considering material, geometry, Reynolds number with air impingement, J. Electron. Packaging 121 (1999) 156–161.
[12] J.G. Maveety, H.H. Jung, Design of an optimal pin-fin heat sink with air impingement cooling, Int. Commun. Heat Mass Transfer 27 (2) (2000) 229–240.
[13] H.A. El-Sheikh, S.V. Garimella, Enhancement of air jet impinging heat transfer using pin-fin heat sinks, IEEE Trans. Compon. Packaging Technol. 23 (2) (2000) 300–308.
[14] J.J. Hwang, C.C. Lui, Detailed heat transfer characteristic comparison in straight and 90-deg turned trapezoidal ducts with pin-fin arrays, Int. J. Heat Mass Transfer 42 (1999) 4005–4016.
[15] J.J. Hwang, C.C. Lui, Measurement of end wall heat transfer and pressure drop in a pin-fin wedge duct, Int. J. Heat Mass Transfer 42 (2002) 877–889.
[16] E. Sansoucy, P.H. Oosthuizen, G.R. Ahmed, An experimental study of the enhancement of air-cooling limits for telecom/datacom heat sink applications using an impinging air jet, J. Electron. Packaging 128 (2006) 166–171.
[17] K.T. Chiang, F.P. Chang, Application of response surface methodology in the parametric optimization of a pin-fin type heat sink, Int. Commun. Heat Mass Transfer 33 (2006) 836–845.
[18] K.T. Chiang, F.P. Chang, T.C. Tsai, Optimum design parameters of pin-fin heat sink using the grey-fuzzy logic based on the orthogonal arrays, Int. Commun. Heat Mass Transfer 33 (2006) 744–752.
[19] H.Y. Li, S.M. Chao, G.L. Tsai, Thermal performance measurement of heat sinks with confined impinging jet by infrared thermography, Int. J. Heat Mass Transfer 48 (2005) 5386–5394.
[20] H.Y. Li, K.Y. Chen, Thermal performance of plate-fin heat sinks under confined impinging jet conditions, Int. J. Heat Mass Transfer 50 (2007) 1963–1970.
[21] H.Y. Li, K.Y. Chen, Thermal-fluid characteristics of pin-fin heat sinks cooled by impinging jet, J. Enhanc. Heat Transfer 12 (2) (2005) 189–201.
[22] S.J. Kim, D.-K. Kim, H.H. Oh, Comparison of fluid flow and thermal characteristics of plate-fin and pin-fin heat sinks subject to a parallel flow, Heat Transfer Eng. 29 (2008) 169–177.
[23] J.S. Issa, A. Ortega, Experimental measurements of the flow and heat transfer of a square jet impinging on an array of square pin fins, J. Electron. Packaging 128 (2006) 61–70.
[24] J.R. Culham, Y.S. Muzychka, Optimization of plate fin heat sinks using entropy generation minimization, IEEE Trans. Compon. Packaging Technol. 24 (2) (2001) 159–165.
[25] W.W. Lin, D.J. Lee, Second-law analysis on a flat plate-fin array under crossflow, Int. Commun. Heat Mass Transfer 27 (2) (2000) 179–190.
[26] S.Z. Shuja, S.M. Zubair, M.S. Khan, Thermoeconomic design and analysis of constant cross-sectional area fins, Heat Mass Transfer 34 (1999) 357–364.
[27] W.A. Khan, J.R. Culham, M.M. Yovanovich, Optimization of pin-fin heat sinks using entropy generation minimization, ITHERM 1 (2004) 259–267.
[28] K. Ogiso, Assessment of overall cooling performance in thermal design of electronics based on thermodynamics, Transactions of the ASME, J. Heat Transfer 123 (2001) 999–1005.
[29] G. Lorenzini, S. Moretti, Numerical analysis on heat removal from Y-shaped fins: efficiency and volume occupied for a new approach to performance optimization, Int. J. Therm. Sci. 46 (2007) 573–579.
[30] P. Naphon, A. Sookkasem, Investigation on heat transfer characteristics of tapered cylinder pin fin heat sinks, Energ. Convers. Manage. 48 (2007) 2671–2679.
[31] G. Ledezma, A. Bejan, Heat sinks with sloped plate fins in natural and forced convection, Int. J. Heat Mass Transfer 39 (9) (1996) 1773–1783.
[32] T.H. Ji, S.Y. Kim, J.M. Hyun, Pressure drop and heat transfer correlations for triangular folded fin heat sinks, IEEE Trans. Compon. Packaging Technol. 30 (1) (2007) 3–8.
[33] S.B. Sathe, B.G. Sammakia, An analytical study of the optimized performance of an impingement heat sink, J. Electron. Packaging 126 (2004) 528–534.
[34] H. Wee, Q. Zhang, P.M. Ligrani, S. Narasimhan, Numerical predictions of heat transfer and flow characteristics of heat sinks with ribbed and dimpled surfaces in laminar flow, Numer. Heat Transfer Part A Appl. 53 (2008) 1156–1175.
[35] A. Shah, B.G. Sammakia, H. Srihari, K. Ramakrishna, A numerical study of the thermal performance of an impingement heat sink-fin shape optimization, IEEE Trans. Compon. Packaging Technol. 27 (4) (2004) 710–717.
[36] A. Shah, B.G. Sammakia, K. Srihari, K. Ramakrishna, Optimization study for a parallel plate impingement heat sink, J. Electron. Packaging 128 (2006) 311–318.
[37] J.P. van Doormaal, F.D. Raithby, Enhancements of the simple method for predicting incompressible fluid flows, Numer. Heat Transfer Part A Appl. 7 (1984) 147–163.
[38] S.V. Patankar, Numerical Heat Transfer and Fluid Flow, McGraw-Hill, New York, 1980.